

Ln₁₈Li₈Rh₅O₃₉ (Ln = La, Pr): a Mixed-Metal Oxide with a Charge-Ordered Arrangement of Rh³⁺ and Rh⁴⁺

Philip P. C. Frampton,[†] Peter D. Battle,^{*,†} and Clemens Ritter[‡]

Inorganic Chemistry Laboratory, Oxford University, South Parks Road, Oxford, OX1 3QR, U.K., and Institut Laue Langevin, 6 Rue Jules Horowitz, BP 156, 38042 Grenoble Cedex 9, France

Received June 13, 2005

Polycrystalline samples of Ln₁₈Li₈Rh₅O₃₉ (Ln = La, Pr) have been synthesized by the ceramic method and characterized by X-ray and neutron diffraction. The compounds crystallize in the cubic space group *Pm* $\bar{3}$ *n*, with *a*₀ ≈ 12.1 Å. The unit cell contains four intersecting <111> chains, each comprised of an alternating sequence of face-sharing RhO₆ octahedra and LiO₆ trigonal prisms. The octahedra located at the points of intersection contain Rh⁴⁺, whereas the remainder contain Rh³⁺; the compounds thus contain a charge-ordered arrangement of the two cations. The polyhedral chains are enclosed in tunnels formed by the Ln–O sublattice. The magnetic properties of the two new compounds are discussed briefly: both are paramagnetic over the temperature range 5 < *T*(K) < 300.

Introduction

It is widely recognized that the electronic properties of a mixed-metal oxide can depend on the degree of order with which different cation species occupy the available crystallographic sites in the adopted structure. The difference between the cations in question might simply be their oxidation state, for example Mn³⁺ and Mn⁴⁺, or they might derive from different elements. The range of behavior observed is exemplified in the former case by the evolution of the magnetic properties of La_{2–x}Sr_xGaMnO₆ with Sr content¹ and in the latter case by the contrast between the magnetic properties of Sr₂FeTaO₆ (disordered Fe³⁺/Ta⁵⁺; spin glass²) and Sr₂FeIrO₆ (ordered Fe³⁺/Ir⁵⁺; antiferromagnet³). We have recently demonstrated that, in the case of perovskite-related *n* = 1 and *n* = 2 Ruddlesden–Popper (RP) structures,⁴ cation ordering can take place in either 2 dimensions (2D)^{5,6} or 3 dimensions (3D),⁷ with significant

consequences for the magnetic properties of the phase. Having observed 2D ordering between Li⁺ and Mn^{*m*+} (*m* = 3 or 4) but 3D ordering between Li⁺ and Ru⁵⁺, we chose to investigate the behavior of RP oxides containing Li⁺ and Rh^{*m*+} (*m* = 3 or 4) in order to ascertain whether ordering is more readily established in these structures when a metal from the second transition series is present. However, our attempts to prepare *n* = 2 La₃LiRhO₇ resulted in the unexpected synthesis of a new, charge-ordered Rh³⁺/Rh⁴⁺ compound, La₁₈Li₈Rh₅O₃₉, and subsequently the Pr analogue Pr₁₈Li₈Rh₅O₃₉. The synthesis and structural chemistry of these two phases are described below.

Experimental Section

The samples described below were prepared by standard high-temperature ceramic synthesis techniques, using high-purity La₂O₃ (99.999%, Alfa), Pr₆O₁₁ (99.996%, Alfa), Rh₂O₃ (99.9%, Alfa), and Li₂CO₃ (99.999%, Alfa) as starting materials. All but Li₂CO₃ were dried at 800 °C prior to use. The oxides were mixed in the appropriate stoichiometric ratio with an excess of the volatile carbonate. The pelletized mixture was contained in an alumina crucible and heated in air. The progress of the reaction was monitored by X-ray powder diffraction, and data suitable for quantitative analysis were collected on the final product using a Siemens D5000 diffractometer operating in Bragg–Brentano

* To whom correspondence should be addressed. E-mail: Peter.Battle@chem.ox.ac.uk.

[†] Oxford University.

[‡] Institut Laue Langevin.

(1) Battle, P. D.; Blundell, S. J.; Claridge, J. B.; Coldea, A. I.; Cussen, E. J.; Noailles, L. D.; Rosseinsky, M. J.; Singleton, J.; Sloan, J. *Chem. Mater.* **2002**, *14*, 425.

(2) Cussen, E. J.; Vente, J. F.; Battle, P. D.; Gibb, T. C. *J. Mater. Chem.* **1997**, *7*, 459.

(3) Battle, P. D.; Blake, G. R.; Gibb, T. C.; Vente, J. F. *J. Solid State Chem.* **1999**, *145*, 541.

(4) Ruddlesden, S. N.; Popper, P. *Acta Crystallogr.* **1957**, *10*, 538.

(5) Burley, J. C.; Battle, P. D.; Gallon, D. J.; Sloan, J.; Grey, C. P.; Rosseinsky, M. J. *J. Am. Chem. Soc.* **2002**, *124*, 620.

(6) Battle, P. D.; Burley, J. C.; Gallon, D. J.; Grey, C. P.; Sloan, J. *J. Solid State Chem.* **2004**, *177*, 119.

(7) Rodgers, J. A.; Battle, P. D.; Dupre, N.; Grey, C. P.; Sloan, J. *Chem. Mater.* **2004**, *16*, 4257.

geometry with Cu $K\alpha_1$ radiation. Data were recorded over the angular range $5^\circ \leq 2\theta \leq 120^\circ$ with $\Delta 2\theta = 0.02^\circ$. Constant-wavelength neutron powder diffraction data were collected at the Institut Laue Langevin (ILL) using the diffractometer D1a. Data were recorded over the angular range $8^\circ \leq 2\theta \leq 146^\circ$, $\Delta 2\theta = 0.05^\circ$ at room temperature using a wavelength of $\lambda = 1.909 \text{ \AA}$. All diffraction data were analyzed by the Rietveld method as implemented in the GSAS program suite.⁸ The magnetization of the reaction products was measured over the temperature range $5 \leq T(\text{K}) \leq 300$ using a Quantum Design MPMS-5 SQUID magnetometer. Data were collected during warmup after cooling in zero applied field (ZFC) and after cooling in the measuring field, which was chosen to be 100 or 1000 Oe as appropriate.

Results

The X-ray diffraction pattern recorded following the attempted synthesis of $\text{La}_3\text{LiRhO}_7$ was dominated not by reflections characteristic of an $n = 2$ RP phase but by a set of Bragg peaks that could be indexed in a body-centered cubic unit cell with $a_0 \approx 12.1 \text{ \AA}$. A search of the Inorganic Crystal Structure Database⁹ suggested that the reaction product might be isostructural with the compound $\text{LaLi}_{0.5}\text{Fe}_{0.2}\text{O}_{2.09}$ (or $\text{La}_{18}\text{Li}_9\text{Fe}_{3.6}\text{O}_{37.62}$) reported previously¹⁰ by Mazza et al. The structure of that material was said to consist of $\langle 111 \rangle$ chains of face-sharing polyhedra in which LiO_6 trigonal prisms alternate with FeO_6 octahedra; four chains cross at the origin and the body-center of the unit cell, and the interchain space is occupied by La^{3+} cations and oxide anions. The results of the original single-crystal structure determination pointed to the composition $\text{La}_{18}\text{Li}_8\text{Fe}_5\text{O}_{39.5}$, but on the evidence of anomalous atomic displacement parameters and the results of a chemical analysis, Mazza et al. preferred to model the structure in space group $Im\bar{3}m$ with only partial occupation of all but the Li site, thus leading to the formula $\text{LaLi}_{0.5}\text{Fe}_{0.2}\text{O}_{2.09}$. In light of this previous investigation, we modified our reaction conditions and the stoichiometry of our reaction mixture until we were able to prepare an apparently pure sample ($\sim 1 \text{ g}$) of the cubic phase. This was achieved by heating a mixture containing Ln, Li, and Rh in a ratio of 18:8:5 at 800°C for 2 h, followed by 11 h at 1000°C , with frequent regrinding of the pellets; extra Li_2CO_3 was added before the final firing to counter the volatility of this reactant. An analogous Pr-containing phase was subsequently prepared by heating at 800°C for 5 h followed by 6 h at 1000°C . The X-ray diffraction data collected on our reaction products were well fitted by the original structural model in space group $Im\bar{3}m$, with fully occupied cation sites and partially occupied anion sites. The apparent formulas of the new compounds could thus be written as $\text{La}_{18}\text{Li}_8\text{Rh}_5\text{O}_{48-\delta}$ and $\text{Pr}_{18}\text{Li}_8\text{Rh}_5\text{O}_{48-\delta}$. The neutron diffraction experiments were undertaken to determine a reliable value of the oxygen content. However, it was immediately apparent from the neutron diffraction data that neither composition adopted the body-centered structure

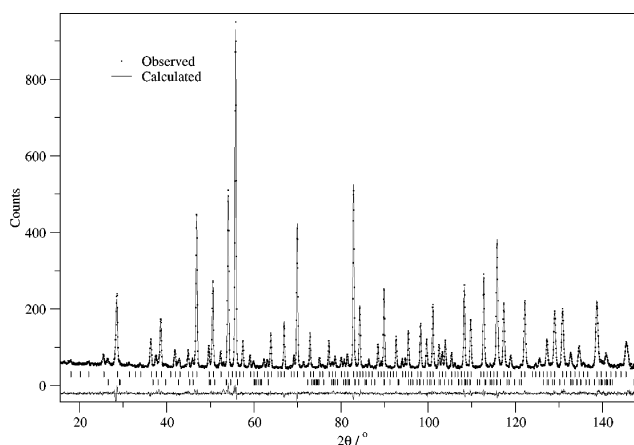


Figure 1. Observed, calculated, and difference neutron powder diffraction patterns of $\text{La}_{18}\text{Li}_8\text{Rh}_5\text{O}_{39}$. Vertical ticks mark reflection positions for both the principal phase and a Li_2CO_3 impurity phase.

described above. The presence of additional Bragg reflections in both cases proved that the cubic lattice was primitive, and the systematic absences indicated the space group $Pm\bar{3}n$. The structures of both compounds could be refined in this space group, and the observed and calculated diffraction profiles are drawn in Figure 1 for $\text{Ln} = \text{La}$. A contribution from a trace ($\sim 1\%$) of unreacted Li_2CO_3 was visible in the data, and this was included as an impurity phase in the data analysis. Our refinements showed that all the possible anion sites identified by Mazza et al. were either vacant or fully occupied with the exception of O4 (48I), the fractional occupancy of which was fixed at a value of 0.25. An anomalously high value of the atomic displacement parameter ($U_{\text{iso}} = 0.0250(7)$) resulted when a fully ordered structure was used to model the La-containing phase with O4 located on the $12f$ site (0.1567(3), 0, 0). The introduction of 4-fold disorder eliminated the anomaly without rendering the least-squares calculation unstable. The parameters defining the occupied sites are listed in Table 1; the same model was used to describe the Pr analogue. The resulting composition of the oxides is thus $\text{Ln}_{18}\text{Li}_8\text{Rh}_5\text{O}_{39}$ ($\text{Ln} = \text{La}$ or Pr). Bond lengths are listed in Table 2. A polyhedral view of the structure is drawn in Figure 2 and the La(Pr) sites are illustrated in Figure 3.

The temperature dependence of the molar magnetic susceptibility of $\text{Ln}_{18}\text{Li}_8\text{Rh}_5\text{O}_{39}$ ($\text{Ln} = \text{La}$ or Pr) is shown in Figure 4. Fitting the data in the temperature range $185 \leq T(\text{K}) \leq 300$ to the Curie–Weiss Law resulted in the following values of the molar Curie constant and Weiss temperature: $\text{Ln} = \text{La}$: $C = 3.31(2) \text{ emu}$, $\theta = -489(4) \text{ K}$; $\text{Ln} = \text{Pr}$: $C = 29.17 \text{ emu}$, $\theta = -58.5 \text{ K}$. The data measured in a field of 1 kG on the La-containing material clearly do not obey the Curie–Weiss Law; an obvious anomaly is observed at $\sim 70 \text{ K}$, and a more subtle change in gradient can be seen at 40 K. Furthermore, the modulus of the Weiss temperature is too large to be physically meaningful. However, the data serve to demonstrate that the compound is paramagnetic and, therefore, that not all the rhodium is present as low-spin $\text{Rh}^{3+}:4d^6$. The data collected in a field of 100 G on the Pr sample appear to follow the Curie–Weiss Law more closely, principally because of the dominant paramagnetic contribution from the Pr^{3+} cations ($J = 4$, C_{calc}

- (8) Larson, A. C.; von Dreele, R. B. *General Structure Analysis System (GSAS)*; Report LAUR 86-748; Los Alamos National Laboratories: Los Alamos, NM, 1990.
- (9) Fletcher, D. A.; McMeeking, R. F.; Parkin, D. *J. Chem. Inf. Comput. Sci.* **1996**, *36*, 746.
- (10) Mazza, D.; Abbattista, F.; Vallino, M. *J. Less Common Met.* **1985**, *106*, 277.

Table 1. Refined Structural Parameters of $\text{Ln}_{18}\text{Li}_8\text{Rh}_5\text{O}_{39}$ (Ln = La or Pr) in Space Group $Pm\bar{3}n$

	Ln	
	La	Pr
a_0 (Å)	12.24595(9)	12.0593(2)
V (Å ³)	1836.44(4)	1753.74(7)
R_{wpr} (%)	3.8	3.8
χ^2	1.7	1.8
Ln1 24 <i>k</i>		
y	0.3079(1)	0.3082(3)
z	0.3044(1)	0.3063(3)
U_{iso} (Å ²)	0.0054(3)	0.0086(7)
Ln2 12 <i>f</i>		
x	0.3463(2)	0.3447(4)
U_{iso} (Å ²)	0.0022(4)	0.001(1)
Rh1 2 <i>a</i>		
U_{iso} (Å ²)	0.003(1)	0.009(2)
Rh2 8 <i>e</i>		
U_{iso} (Å ²)	0.0074(6)	0.0112(9)
Li 16 <i>i</i>		
x	0.3759(4)	0.3749(6)
U_{iso} (Å ²)	0.019(2)	0.016(3)
O1 48 <i>l</i>		
x	0.8627(1)	0.8638(2)
y	0.8598(1)	0.8616(2)
z	0.6934(1)	0.6910(2)
U_{iso} (Å ²)	0.0064(3)	0.0063(4)
O2 6 <i>d</i>		
U_{iso} (Å ²)	0.010(1)	0.013(1)
O3 12 <i>g</i>		
x	0.6325(2)	0.6310(4)
U_{iso} (Å ²)	0.0053(7)	0.017(1)
O4 12 <i>f</i> (48 <i>l</i>)		
x	0.1569(2)	0.1590(3)
y	0.012(1)	0.011(2)
z	0.0146(9)	0.011(2)
U_{iso} (Å ²)	0.0055(2)	0.0059(3)

Table 2. Bond Lengths (Å) in $\text{Ln}_{18}\text{Li}_8\text{Rh}_5\text{O}_{39}$ (Ln = La or Pr)^a

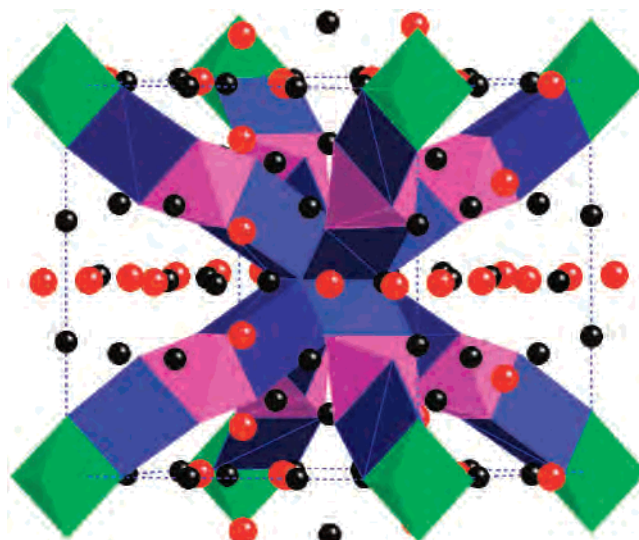
	Ln	
	La	Pr
Ln1–O1	2.671(3) 2.655(3) 2.554(2) × 2 2.655(3) 2.671(3)	2.644(5) 2.625(5) 2.491(2) × 2 2.625(5) 2.644(5)
Ln1–O2	2.498(2)	2.440(5)
Ln1–O3	2.476(2) 3.156(3)	2.434(4)
Ln2–O1	2.451(1) × 4	2.381(2) × 4
Ln2–O3	2.486(2) × 2	2.450(4) × 2
Ln2–O4	2.331(3)	2.247(5)
Rh1–O4	1.935(3) × 6	1.927(4) × 6
Rh2–O1	2.048(1) × 6	2.050(2) × 6
Li–O1	2.250(6) × 3	2.228(8) × 3
Li–O4	2.118(1)* × 3	2.115(2)* × 3
Li–Li	3.04(1)	3.02(1)
Rh1–Li	2.632(9)	2.61(1)
Rh2–Li	2.671(9)	2.61(1)

^a The asterisk denotes an average of 4 Li–O bonds as the oxygen position is disordered.

= 1.60 emu/mol of Pr^{3+}). No anomaly is observed at 70 K in this case, but the gradient change at lower temperature is again apparent.

Discussion

The structures refined in this study are similar to that proposed previously for $\text{LaLi}_{0.5}\text{Fe}_{0.2}\text{O}_{2.09}$, in that they do involve $\langle 111 \rangle$ polyhedral chains in a matrix of Ln^{3+} and oxide ions. However, there are a number of important differences

**Figure 2.** Polyhedral view of the structure of $\text{Ln}_{18}\text{Li}_8\text{Rh}_5\text{O}_{39}$: Rh1O_6 and Rh2O_6 octahedra are colored green and purple, respectively, LiO_6 prisms are blue. Red and black circles represent O and Ln, respectively.

in the structural models, many of which stem from the decision by Mazza et al. to assign the composition of their single crystal on the basis of a chemical analysis of the material from which the crystal was extracted. The enhanced sensitivity of neutron diffraction in the location of light atoms has allowed us to carry out a full structural characterization of the rhodium analogues and to clarify a number of issues. Most importantly, our compounds are stoichiometric with all the crystallographic sites fully occupied with the exception of O4, where we have introduced 4-fold disorder to model local atomic displacements. Our data analysis brings to light a number of chemically interesting features. The alternation of octahedral and prismatic geometry along a chain is strongly reminiscent of the $A_3A'BO_6$ phases,¹¹ for example, $\text{Sr}_3\text{LiRuO}_6$,¹² Sr_4RhO_6 ,¹³ ($A = A' = \text{Sr}$), and $\text{Ca}_3\text{Co}_2\text{O}_6$,¹⁴ ($A' = B = \text{Co}$), which have been the focus of much recent research work. These compositions are the simplest ($m = 0$, $n = 1$) members of the family $A_{3n+3m}A'_nB_{3m+n}O_{9m+6n}$ (sometimes written $A_{1+x}(A'_xB_{1-x})O_3$ where $x = n/(3m + 2n)$) in which polyhedral chains made up of $A'O_6$ prisms and BO_6 octahedra in the ratio $n:3m+n$ are separated from each other by space-filling A cations. The latter are usually alkaline earths; no compound having lanthanide cations on this site has been prepared. Rhodium has previously been found in both the octahedral and the prismatic sites in these compounds, for example,¹⁵ in $m = 1$, $n = 1$ $\text{Sr}_6\text{Rh}_5\text{O}_{15}$ in which tetramers of octahedra are separated by a single prism. This is clearly a mixed-valence compound, although there is no ordering of the different oxidation states over the different crystallographic sites; a similar situation was observed¹⁶ in $m = 2$, $n = 1$ $\text{Ba}_9\text{Rh}_8\text{O}_{24}$. The oxidation states involved in these two examples are expected to be Rh^{3+} and Rh^{4+} , which

(11) Stitzer, K. E.; Darriet, J.; Zur Loye, H. C. *Curr. Opin. Solid State Mater. Sci.* **2001**, 5, 535.

(12) Darriet, J.; Grasset, F.; Battle, P. D. *Mater. Res. Bull.* **1997**, 32, 139.

(13) Vente, J. F.; Lear, J. K.; Battle, P. D. *J. Mater. Chem.* **1995**, 5, 1785.

(14) Fjellvag, H.; Gulbrandsen, E.; Aasland, S.; Olsen, A.; Hauback, B. C. *J. Solid State Chem.* **1996**, 124, 190.

(15) Claridge, J. B.; Zur Loye, H. C. *Chem. Mater.* **1998**, 10, 2320.

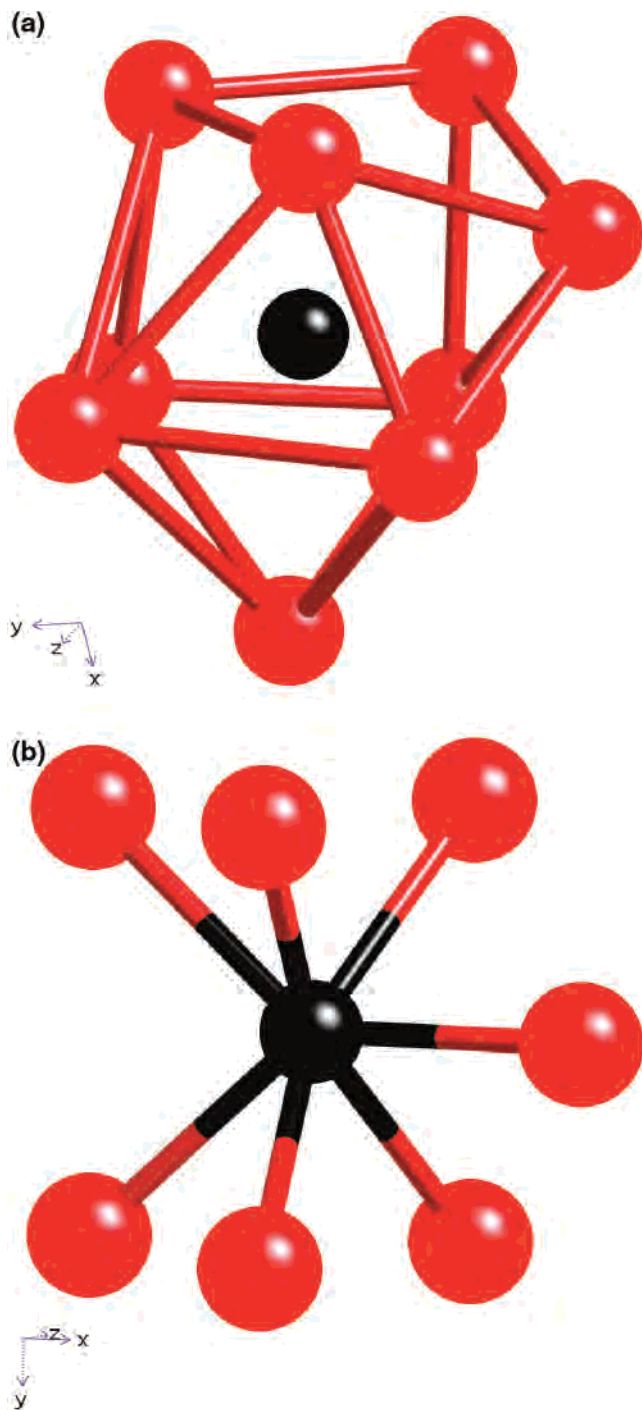


Figure 3. The local environment of (a) Ln1 and (b) Ln2.

have both been observed in single-valence compositions, for example, $\text{Sr}_3\text{LnRhO}_6$ ¹⁷ ($\text{Ln} = \text{Sm}, \text{Eu}, \text{Tb}, \text{Dy}, \text{Ho}, \text{Er}, \text{Yb}$) and Sr_4RhO_6 .¹³ There has also been a report¹⁸ of Rh^{5+} occurring in Sr_3ARhO_6 ($\text{A} = \text{Li}, \text{Na}$). A simple survey of Rh–O bond lengths within this structural family shows a progression in typical values from ~ 2.07 (Rh^{3+}) to ~ 2.03 (Rh^{4+}) and 1.99 Å (Rh^{5+}), but a closer inspection reveals a

(16) Stützer, K. E.; Smith, M. D.; Darriet, J.; Zur Loye, H. C. *Chem. Commun.* **2001**, 1680.

(17) Layland, R. C.; Kirkland, S. L.; Zur Loye, H. C. *J. Solid State Chem.* **1998**, *139*, 79.

(18) Reisner, B. A.; Stacy, A. M. *J. Am. Chem. Soc.* **1998**, *120*, 9682.

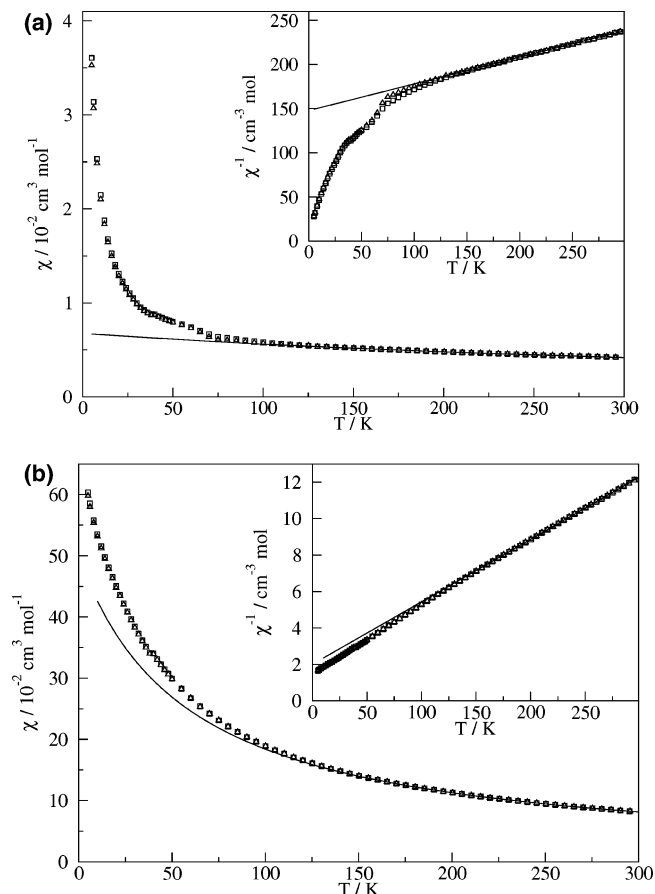


Figure 4. Temperature dependence of the molar magnetic susceptibility of $\text{Ln}_{18}\text{Li}_8\text{Rh}_5\text{O}_{39}$: (a) $\text{Ln} = \text{La}$, (b) $\text{Ln} = \text{Pr}$. Δ (\square) represent data collected after zero-field cooling (field cooling). A fit to the Curie–Weiss Law is shown.

more-complex situation. First, the mean Ru^{4+} –O bond length in RuO_2 is 1.97 Å,¹⁹ and that in SrRuO_3 is 1.983 Å,²⁰ the mean Ru^{5+} –O distance in $\text{La}_2\text{LiRuO}_6$ is 1.953 Å.²¹ Given that Rh^{m+} would be expected to be smaller than Ru^{m+} , these data suggest that the cation environment in $\text{A}_{1+x}(\text{A}'_x\text{B}_{1-x})\text{O}_3$ phases is relatively relaxed and that the values quoted above lie at the upper end of the range of Rh^{m+} –O distances. Many $\text{A}_{1+x}(\text{A}'_x\text{B}_{1-x})\text{O}_3$ compositions are incommensurate and must be described using 4-dimensional crystallography. In these cases, only a range of Rh–O distances can be defined, and in $\text{Ba}_{1+x}\text{Cu}_x\text{Rh}_{1-x}\text{O}_3$ ($x = 0.1605$), that range was²² 1.763 – 2.088 Å; the lower bound is clearly much shorter than the bond lengths cited above, and the data from the incommensurate phases thus support our hypothesis that the Rh–O bonds in the simpler structures are relaxed. The composition $\text{Ln}_{18}\text{Li}_8\text{Rh}_5\text{O}_{39}$ is consistent with a 4:1 ratio of Rh^{3+} and Rh^{4+} . We postulate that the $8e$ sites ($\text{Rh}2\text{–O}1 \approx 2.05$ Å) are occupied by Rh^{3+} and the smaller $2a$ sites ($\text{Rh}1\text{–O}4 \approx 1.93$ Å) by Rh^{4+} to form a fully charge-ordered structure. The bond length at the former site is in good

(19) Boman, C. E. *Acta Chem. Scand.* **1970**, *24*, 116.

(20) Jones, C. W.; Battle, P. D.; Harrison, W. T. A. *Acta Crystallogr. C* **1989**, *45*, 365.

(21) Battle, P. D.; Grey, C. P.; Hervieu, M.; Martin, C.; Moore, C. A.; Paik, Y. J. *Solid State Chem.* **2003**, *175*, 20.

(22) Zakhour-Nakhl, M.; Claridge, J. B.; Darriet, J.; Weill, F.; Zur Loye, H. C.; Perez-Mato, J. M. *J. Am. Chem. Soc.* **2000**, *122*, 1618.

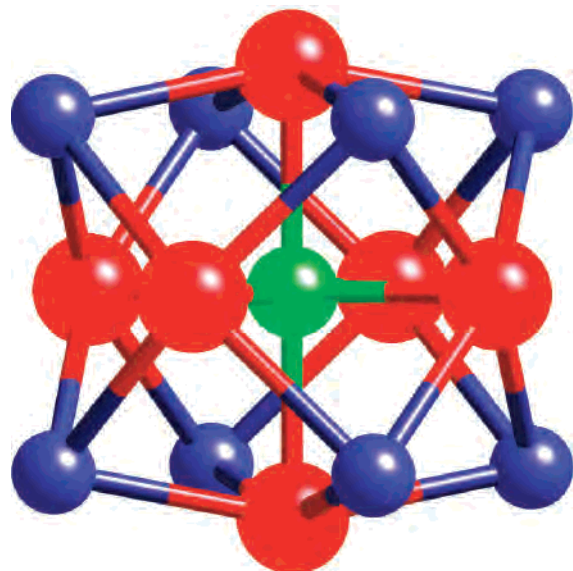


Figure 5. The local environment around Rh1; the O4 atoms (red circles) are drawn in an ordered array.

agreement with the expected value, whereas the Rh1–O distance at the latter site lies within the range reported previously but is clearly shorter than that in many other Rh^{4+} compounds. The Rh1 site is illustrated in Figure 5, which emphasizes the high atomic density in the region where the $\langle 111 \rangle$ polyhedral chains intersect. Fourteen atoms lie within 2.65 \AA of Rh1, $6 \times \text{O4}$ and $8 \times \text{Li}$; the shortest Li–Li distance (3.04 \AA , the same as in lithium metal) occurs in this part of the structure. The introduction of disorder at the O4 site serves to lengthen the Rh1–O bond length and thus relaxes the environment somewhat. Nevertheless, the Rh^{4+} environment is significantly more crowded than that in $\text{Sr}_4\text{-RhO}_6$, where only six oxide ions lie within 2.9 \AA of the Rh^{4+} cation, and it is therefore not surprising to observe a relatively short Rh^{4+} –O bond length. The Li–O distances within the trigonal prismatic site are very similar to the values reported¹² for A_3LiRuO_6 ($\text{A} = \text{Ca}, \text{Sr}$) but are relatively large for six-coordinate Li^+ ($\text{Li}-\text{O} \approx 2.08 \text{ \AA}$ in $\text{La}_2\text{LiRuO}_6$). The enhanced atomic displacement parameters of Li^+ presumably reflect the presence of static disorder that occurs on this sublattice in response to that on the O4 sublattice. The lanthanide cations are found in two distinct environments; Ln1, occupying the $24k$ site, lies within a distorted, face-capped square antiprism, whereas Ln2, occupying the $12f$ site, lies within a trigonal prism, one rectangular face of which is capped by an oxide ion to generate a relatively short Ln–O distance (2.31 \AA). However, it is more informative to consider the Ln environment over larger distances. The atoms O1 and O4 are bonded only to Li and Rh, with O2 and O3 being bonded only to Ln. This facilitates a description of the structure in terms of two substructures: first, the $\langle 111 \rangle$ polyhedral chains which involve Rh1, Rh2, Li, O1, and O4 and, second, the network built up of Ln1, Ln2, O2, and O3. This network is illustrated in Figure 6. When considered in this manner, the structure begins to resemble a microporous solid, with the polyhedral chains running through tunnels in a lanthanide–oxide network. Each unit cell contains four intersecting tunnels which run along $\langle 111 \rangle$ directions, and

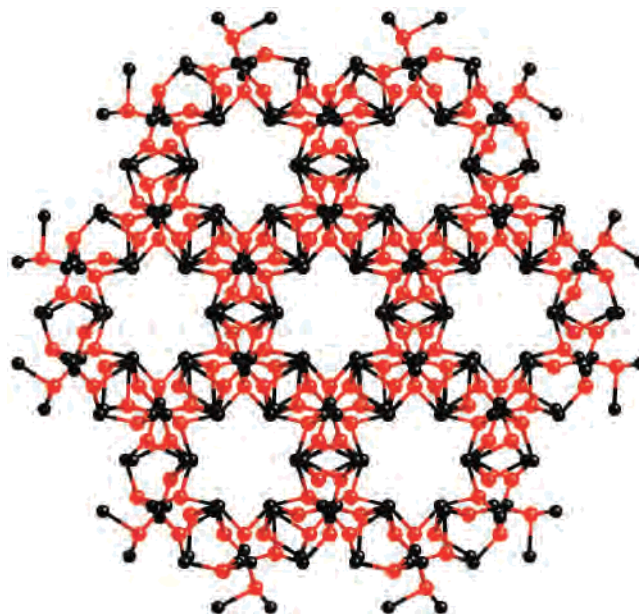


Figure 6. $\langle 111 \rangle$ projection of the network formed by Ln1, Ln2, O3, and O4.

the Rh^{4+} cations are located at the points of intersection. Each tunnel is defined by a 12-membered ring formed by alternating Ln and O2 atoms, with the cations being directed into the tunnel to enhance their interaction with the sheath of negative charge with which O1 and O4 encircle the Li–Rh–Li chains. The Ln–Ln distance across the diameter of the tunnel is 6.425 \AA for $\text{Ln} = \text{La}$, and the shortest La–La distance in the structure is 3.58 \AA .

The study described above provides clear evidence for charge ordering between Rh^{3+} and Rh^{4+} in two new, stoichiometric mixed-metal oxides. The only previous report²³ of such charge ordering relates to $\text{Pb}_3\text{Rh}_7\text{O}_{15}$, which was described, on the basis of bond-valence calculations, as containing two Rh^{3+} sites, one Rh^{4+} site, and one mixed-valence $\text{Rh}^{3.5+}$ site. The variation in bond lengths ($2.04(1)$ and $2.06(2)$, $2.00(1)$, and $2.01(1) \text{ \AA}$, respectively) was certainly less marked than in the present case, and it is not clear that the bond valence parameters for unusual oxidation states such as Rh^{4+} are well defined. The difference between the two Rh–O bond lengths in $\text{Ln}_{18}\text{Li}_8\text{Rh}_5\text{O}_{39}$ is more significant, with the Rh1–O4 distance within the 14-atom cage being particularly short, and the evidence for charge order is thus more convincing. The observation of paramagnetism in $\text{La}_{18}\text{Li}_8\text{Rh}_5\text{O}_{39}$ (Rh^{4+} , $S = 1/2$) is also consistent with our suggestion of a charge-ordered structure, but the behavior of the magnetic susceptibility in the temperature range $40 \leq T(\text{K}) \leq 70$ shows that these compounds cannot be described in terms of isolated, localized-electron paramagnetic centers. More experimental work will have to be undertaken before the electronic structure can be fully understood.

Acknowledgment. We are grateful to the EPSRC for the provision of a studentship to P.P.C.F.

IC050949S

(23) Omary, J.; Kohlmüller, R.; Batail, P.; Chevalier, R. *Acta Crystallogr. B* 1980, 36, 1040.